Atomic-resolution study of overlayer formation and interfacial mixing in the interaction of phosphorus with Si(001)

Yajun Wang, Xiangxiong Chen, and Robert J. Hamers*
Department of Chemistry, University of Wisconsin, 1101 University Avenue, Madison, Wisconsin 53706
(Received 24 January 1994)

Scanning tunneling microscopy (STM), tunneling spectroscopy, and Auger-electron spectroscopy have been used to study the formation of phosphorus-terminated silicon (001) surfaces by the thermal decomposition of phosphine (PH_3). The STM images show that surface phosphorus atoms readily displace Si from the substrate, dramatically changing the overall surface morphology through the formation of large numbers of islands and an extreme roughening of step edges. The surfaces are terminated with P—P dimers, but also contain large numbers of line defects which act as a strain relief mechanism. STM images are used to determine the symmetry of these line defects and are compared with model defect structures. Line defects in the phosphorus-terminated surface both nucleate islands and also constrain their growth in one dimension, such that the phosphorus-terminated surfaces contain large numbers of extremely anisotropic islands and very rough step edges. At lower phosphorus coverage, the STM experiments are able to identify Si and P atoms individually, revealing the formation of large numbers of Si—P heterodimers and the simultaneous disappearance of the strain-induced line defects. Counting statistics are used to study the equilibrium between Si=Si, Si—P, and P—P dimers, showing that the surface is a nearly random alloy with a slight nonstatistical preference for formation of the Si—P heterodimer. The geometric and electronic properties of Si=Si, Si—P, and P—P dimers on Si(001) are discussed on the basis of tunneling microscopy and tunneling spectroscopy measurements.

I. INTRODUCTION

Phosphorus is a common dopant used in the fabrication of *n*-type silicon, usually introduced in chemical vapor deposition (CVD) processes through the decomposition of phosphine, PH_3. Several studies have shown that during the growth of silicon from chemical precursors such as silane, small amounts of PH_3 strongly influence the growth kinetics, decreasing the Si growth rate far out of proportion to the PH_3 concentration in the gas stream.[1-5]

In the last several years, there has been a great interest in the use of surfactants to control surface stress in the growth of heterointerfaces, most notably the growth of Ge on Si using As or Sb as surfactants.[6-12] While deposition of Ge on pure Si produces three-dimensional island growth after three monolayers due to the 4.3% lattice mismatch between Ge and Si, Copel and co-workers[6,7] have shown that incorporation of arsenic or antimony as surfactants during growth stabilizes the surface against three-dimensional growth by controlling the surface tension. Using this surfactant growth technique, they were able to grow Ge overlays of arbitrary thickness on Si without forming islands. Since phosphorus is a group V element isoelectronic with both As and Sb, phosphorus might be expected to show similar surfactant properties.

Interfacial mixing plays an important role both in the use of adlayers of group V elements as surfactants as well as the incorporation of these elements into the crystal lattice as dopants. In the particular case of arsenic, it is known that As—As dimers can form atop a Si substrate or can displace silicon to form As—As dimers in the surface plane, depending on the preparation conditions.[13,14] Tromp, Denier van der Gon, and Reuter[9] have suggested that the tendency toward displacive adsorption vs simple adsorption depends on how the surface free energy varies as a function of coverage. In the analysis of Tromp, as well as most other studies of surfactant growth, it is usually assumed that the surface contains As—As dimers and Si—Si dimers, but heterodimers such as Si—P or Si—As have not been widely considered. However, Yu and Oshiyama[15] recently suggested that heterodimers may play an important role in surface doping. Because of the different electronic structures of group IV and group V elements, it should be possible with scanning tunneling microscopy (STM) to investigate the composition of such overlayers and to determine whether in fact such heterodimers are present and, if present, whether they play any role in the surface energetics or growth kinetics.

Despite its widespread use as a dopant and its potential as a surfactant, the adsorption of phosphorus on Si(001) has not been extensively studied. Yu, Meyerson, and co-workers[5,16,17] performed the most extensive studies, using Auger-electron spectroscopy, x-ray photoelectron spectroscopy, temperature-programmed desorption, and low-energy electron diffraction (LEED) to investigate the adsorption and dissociation of phosphine (PH_3) on the Si(001) surface. They found that at temperatures higher than 675 K (the desorption temperature of H_2), exposure to PH_3 produced a phosphorus-terminated surface with a coverage of approximately one monolayer, and which showed a streaky (2×1) LEED pattern. They proposed that phosphorus-phosphorus dimers formed on the surface and passivated it against further chemical reaction, thereby decreasing CVD growth rates. They also found that phosphorus was not effective in doping the surface

region until the surface P coverage was very close to one monolayer, at which point the Fermi level suddenly jumped by 0.45 eV to near the conduction band. At sufficiently high temperatures they found that phosphorus desorbed from the surface, mostly in the form of P_2.

In this work, we report on STM investigations of the atomic structure of phosphorus overlayers on silicon formed by the thermal decomposition of PH_3. We find that phosphorus readily displaces silicon from the substrate, resulting in extensive island formation. Because of the different electronic structures of Si=Si, Si—P, and P—P dimers, we are able to identify these three kinds of dimers on the surface and are able to study the chemical composition of the surface on an atom-by-atom basis. For the P—Si system, we find that the chemical composition of surfaces produced by adsorption of phosphorus onto clean Si(001) as well as surfaces produced by desorption of phosphorus from the P-terminated surface both consist of nearly random alloys of P and Si, but with a slightly nonstatistical preference for formation of the P—Si heterodimer. As a result, over a wide range of phosphorus coverages the dominant chemical specie on the surface is the Si—P heterodimer. Our results also show the stress-induced line defects occur in this system at saturation coverage where P—P dimers dominate, but not at lower coverage where Si—P dimers dominate. Based on the symmetry of the line defects with respect to the underlying crystal lattice, we show that these line defects cannot be the same defects recently proposed by Tersoff[12] to account for similar-appearing line defects in the growth of strained Ge films on Si(001). We also show that the line defects present on the P-terminated surface significantly modify the mechanisms of island nucleation and growth.

II. EXPERIMENTAL

STM experiments were performed in an ultrahigh vacuum chamber with a base pressure of below 1×10^{-10} torr. Wafers of *n*-type Si(001) oriented to within 0.5° obtained from Wacker Chemitronic were used. Samples were prepared by first degassing for about 10 h at 900 K, then annealing to 1400 K for several seconds on a separate heating stage. Temperatures were measured using an infrared pyrometer. After allowing 30 min for cooling to room temperature, samples were transferred to the STM and imaged to ensure that the starting surfaces were clean and well ordered. Average terrace widths of nearly 1000 Å were measured in the STM, with atomic-resolution images showing surface structure commensurate with previous studies.[18–20] Phosphorus overlayers were prepared from the *in situ* thermal decomposition of high-purity PH_3 (99.999%, Matheson). After imaging the clean silicon surface to ensure that the starting surfaces were clean and well ordered, the silicon samples were moved to the heating stage, heated to a controlled temperature of approximately 820 K, and then exposed to PH_3 admitted into the vacuum chamber through a leak valve. The samples were then cooled, moved back to the STM tunneling stage, and imaged at room temperature. All images were acquired in the "constant-current" mode of operation using tunneling currents (I_t) of less than 1.0 nA with the sample bias (V_{sample}) between −3 V (probing occupied surface states) and +3 V (probing unoccupied surface states), as indicated in the figure captions. Tunneling spectroscopy measurements were performed by interrupting the STM feedback system and ramping the sample-tip bias while keeping the sample-tip separation constant.[21]

III. RESULTS

A. Structure and properties of phosphorus overlayers near monolayer coverage

Yu and co-workers showed that phosphine decomposition on Si(001) is temperature dependant. At low temperatures the maximum coverage is approximately 0.25, due to the presence of surface hydrogen from the PH_3 decomposition. Between 675 and 825 K the coverage increases, reaching a maximum of one monolayer near 825 K, and decreasing again at $T > 875$ K due to phosphorus desorption. Figures 1–3 show STM images at successively higher resolution of surfaces prepared by heating a clean, well-ordered Si(001) surface to 825 K, exposing the surface to 10^{-7} torr PH_3 for 200 s (total exposure of 20 L, where 1 L$=10^{-6}$ torr-s), and then cooling the sample back to 300 K under ultrahigh-vacuum conditions. Figure 1(a) shows an STM image of a 1200×1150 Å^2 region of the surface, revealing the overall surface morphology on a large scale. This image includes parts of five different terraces, with the highest terrace, labeled "1" at the extreme upper right and the lowest terrace, labeled "5," at lower left. Examination of this image shows that exposure to PH_3 induces three dramatic changes in the overall surface morphology. The first morphological change produced by PH_3 exposure is the creation of a large number of long, narrow islands on the terraces, whereas the starting surface consisted of flat terraces separated by monatomic steps. The second morphological change created by PH_3 exposure is the extreme roughening of the step edges, with fingerlike extensions and deep invaginations extending nearly the width of the individual terraces. The third morphological change produced by PH_3 exposure is the creation of very long, one-dimensional defects which appear as dark, narrow lines, particularly visible on terraces 1 and 3. These line defects will be denoted as "LD," and several LD defects are indicated in Fig. 1(a). Although they are most apparent in Fig. 1(a) on terraces 1 and 3, these line defects can be observed on all terraces, but a slightly asymmetric STM tip makes the defects more apparent on some terraces and not on others due to the 90° rotation of the crystal structure across a monatomic step on Si(001).

Figure 1(b) shows that on distance scales of several hundred Å, the terrace structure becomes dominated by the islands, and it becomes difficult to identify a single "substrate" terrace. In some cases the islands are only the width of a single dimer row. We refer to such islands as "dimer strings" (DS) and have indicated several examples in Fig. 1(b). In this figure, it can be seen that the is-

lands, particularly the islands visible to upper right, are bounded on their long sides by line defects in the underlying layer. This is true irrespective of the size of the island. Individual dimer strings always have a line defect on one side along their long dimension, while larger islands (easily visible at upper right and at lower left) are always bounded on both sides by line defects. The large number of very asymmetric islands also results in the formation of a large number of apparent holes in the surface, which typically extend only one atomic layer deep. These holes are also asymmetric in the same direction as the island and are most likely produced by the imperfect intersection of two islands under conditions where atoms do not diffuse over the islands to "fill in" the hole. One example of such a hole is labeled "H" in Fig. 1(b). Finally, we note that the extreme degree of step roughing and island formation in some cases leads to the spontaneous formation of small regions of double-height steps, several examples of which are labeled "2S" in Fig. 1(b). In large-scale images such as Figs. 1 and 2, we find that comparatively smooth step edges alternate with rougher step edges, in a manner similar to that of the clean Si(001) surface. In all cases, we find that the dimer rows of PH_3-exposed surfaces run parallel to the smooth step edges, and at double steps [as in Fig. 1(b)] the dimer rows run perpendicular to the double-height step edge. This indicates that the observed structures are not simply a phosphorus adlayer, but in all cases involve substitution of phosphorus for silicon in the outermost atomic layer.[13,14] While in principle the amount of phosphorus ejection

FIG. 1. (a) Large-scale STM image of phosphorus-terminated Si(001) surface, showing spontaneous island formation and the presence of line defects cutting perpendicular to the dimer rows. "1" denotes highest terrace, "5" the lowest. $V_{sample} = -2.0$ V, $I_{tunnel} = 0.2$ nA, Dimensions are 1150×1200 Å^2. (b) STM image of P-terminated Si(001) surface. Note the dimer string (DS) nucleated adjacent to a line defect and other islands at upper right bounded on their long sides by line defects. "1" denotes the highest terrace, "4" the lowest. "2S" denotes double-height step. $V_{sample} = -2.0$ V, $I_{tunnel} = 0.2$ nA; Dimensions are 675×710 Å^2.

FIG. 2. (a) High-resolution STM image showing detailed appearance of upper and lower terraces, and nucleation of islands adjacent to line defects. Note the "specked" appearance of the surface due to admixture of P and Si atoms on both the islands and the underlying substrate. $V_{sample} = -2.0$ V, $I_{tunnel} = 0.2$ nA. Dimensions are 340×365 Å^2. (b) Atomic-resolution STM image showing detailed appearance of line defects and the characteristic appearance of P—P dimers and P—Si dimers. The highest terrace is labeled "1," the main large terrace labeled "2," and the lowest terrace is labeled "3." $V_{sample} = -2.0$ V, $I_{tunnel} = 0.2$ nA. Dimensions are 173×170 Å^2.

could be calculated by obtaining STM images on extremely flat surfaces and measuring the fractional island coverage, this is not possible because even on our extremely flat starting surfaces, which have average step separations of nearly 1000 Å, the extremely rough step edges make it impossible to distinguish "islands" from step-edge roughness.

Figures 2(a) and 2(b) show images of the surfaces prepared in the same manner as in Fig. 1, at successively higher resolution. Figure 2(a) consists of two terraces. In Fig. 2(b), three planes are visible, labeled 1–3, with the highest terrace (1) consisting of only two rows of dimerized atoms. At the resolution of Figs. 2(a) and 2(b), we are able to observe in more detail the structure of the line defects, the nucleation site for islands, and the internal structure of the surface unit cell. In Fig. 2(a), rows can be observed on the upper terrace, and line defects can be observed on both the upper and lower terraces. On the larger, lower terrace these defects extend for hundreds of Å with only occasional shifts in direction. An examination of the dimer rows on each side of these line defects (most easily visible by looking at the islands) shows that in almost all instances the dimer rows on each side of the line defect have the same phase (i.e., the troughs between dimer rows on opposite sides of the line defect are collinear). This shows that the line defects are not the "antiphase" defects that have previously been observed in silicon homoepitaxy.[22,23] In Fig. 2(b) at upper left, we can see a good example of line defects in which the dimer rows on opposite sides are in phase and out of phase; these regions are necessarily separated by an "AP1" antiphase boundary which involves a translation shift of 3.84 Å parallel to the dimer bond direction (perpendicular to the dimer rows), and appears similar to the AP1 boundaries observed in silicon homoepitaxy.[22,23] The in-phase and out-of-phase line defects appear to have similar structures, and we will henceforth simply refer to them collectively as line defects (LD).

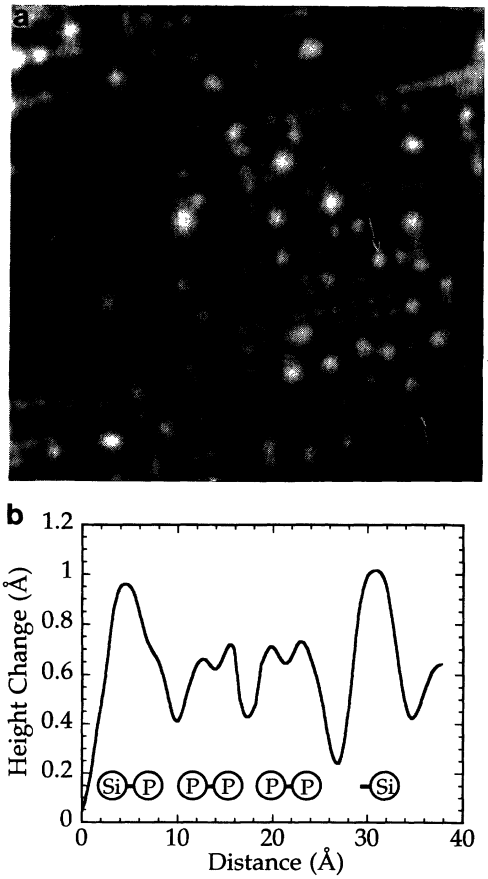

FIG. 3. (a) Enlarged image from Fig. 2(b), showing the appearance of P—P dimers as individual atoms, and showing that in Si—P dimers the Si atom appears as a high protrusion on one side of the dimer, with 50% probability of being found on either side. $V_{sample} = -2.0$ V, $I_{tunnel} = 0.2$ nA. Dimensions are 92×92 Å^2. (b) Height profile measured between the arrows indicated in Fig. 3(a), showing that P=P dimers appear as two protrusions with maxima separated by 3.2 Å, and Si "dangling bonds" on Si—P dimers appear about 0.3 Å higher.

As noted earlier, these line defects appear to act as nucleation sites for next-year growth. In Fig. 2(a), there are several examples in which dimer strings have nucleated adjacent to (but not on top of) line defects. The dimer string at the bottom right in Fig. 2(a) is bounded on *both* sides by line defects. Similarly, at higher resolution Fig. 2(b) shows that the two dimer rows constituting the topmost terrace are bounded on both sides by line defects. Surprisingly, in Fig. 2(a) we see that the dimer strings at bottom right and at left center appear to cross the gap between islands, forming a bridge only a single dimer wide between the islands.

In Fig. 2(b) and particularly in Fig. 3(a), the internal structure of the surface unit cell can be resolved. Like the clean Si(001) surface, the surface unit cell of these surfaces has a (2×1) periodicity, but with an internal structure substantially different from that of the clean surface. At negative sample bias (probing occupied surface states), the STM images show that each (2×1) unit cell is clearly resolved into two protrusions. In contrast, under identical conditions STM images of the clean Si(001) surface show bean-shaped dimers having only a single maximum in the center of the unit cell, due to the fact that the electrons tunnel primarily from a delocalized π bonding orbital shared between the two Si atoms.[18,19,24] Thus, the dimers in Fig. 3(a) are clearly distinguishable from Si=Si dimers and are attributed to P—P dimers on a bulklike Si(001) surface. Close inspection of Fig. 3(a) also shows that the white protrusions are always located one side or the other of the dimer (50% probability for each side), and appear as though the two atoms constituting a single dimer have different chemical identity (and hence, different electronic structures). Through controlled studies as a function of coverage and temperature, some of which are described below, we conclude that the "bright" sites observed in Fig. 3 arise from Si—P heterodimers in which the lower (darker) atom is phosphorus and the higher (brighter) atom is silicon. Thus, the phosphorus-terminated surfaces observed in Figs. 1–3 consist primarily of P—P dimers, with occasional P—Si dimers.

The height changes measured under constant-current

STM tunneling across the P—P and Si—P dimers are shown more quantitatively in Fig. 3(b), which shows the measured height change along a line between the unmarked arrowheads in Fig. 3(a). The line profile shows that P—P dimers give rise to two protrusions 3.2±0.1 Å apart separated by a minimum of 0.10 Å deep, and that the bright features are about 0.3 Å higher than the surrounding dimers. Since the STM primarily probes the valence electronic structure, we also attempted to obtain atomic-resolution images of the P-terminated surfaces at positive bias, to identify the spatial location of the unoccupied surface states. Under positive-bias conditions, we found it extremely difficult to obtain stable tunneling, even at currents as low as 20 pA. Furthermore, when we did succeed in getting stable tunneling the surface showed very little corrugation. However, we were able to determine that the protrusions observed at negative bias and attributed to the Si "dangling bonds" of Si—P dimers also appear as protrusions at positive bias, consistent with this overall picture.

Figure 4 depicts the structures of Si=Si, P—P, and P—Si dimers atop the Si(001) surface. In order to facilitate the discussion section, we have also included approximate bond lengths based on literature data for dimerized silicon surface and for inorganic silicon-phosphorus compounds, as discussed below.

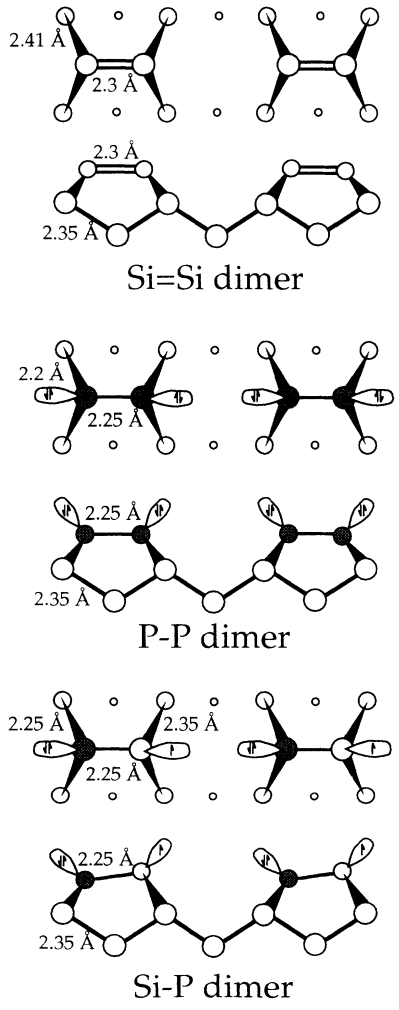

FIG. 4. Structural models for Si=Si, P=P, and Si—P dimer, including top and side views. Bond lengths are taken from the literature as described in the text.

In order to help identify the nature of the line defects, we also measured corrugation profiles across the line defects, parallel to the dimer rows. STM images such as Fig. 2(b) show that the line defects appear as if the two dimers have been pulled in toward the bulk and slightly separated, resulting in the formation of a narrow gap between them. Figure 5 shows the height profile across such a defect, measured between the arrows shown in Fig. 2(b). The most important result to be emphasized here is that the total width of the defect is only two dimers wide, with the defect having a symmetry plane which passes midway *between* two dimers of the surface plane, and passes *through* the second-layer atom. This structure is included in a schematic fashion in Fig. 5 to better illustrate the symmetry of the defects. As will be discussed later, the basic symmetry of the defect can be used to discriminate between structural models for these defects.

We have also characterized the surfaces shown in Figs. 1–3 using Auger-electron spectroscopy for elemental analysis and using tunneling spectroscopy to probe the valence electronic structure of the surface. In Fig. 6(a), the Auger spectrum shows a large silicon peak at 92 eV and a large phosphorus peak at 121 eV, with a peak ratio of approximately 0.57, demonstrating a large amount of phosphorus within the outermost 10 Å of the surface, most of which we attribute to phosphorus forming P_2 dimers on the surface.

Figure 6(b) shows the results of tunneling spectroscopy measurements made on the surfaces before and after preparation of the phosphorus overlayer as described in Fig. 1. For these measurements, the sample-tip distance as regulated using a sample voltage of −1.5 V and a tunneling current of 800 pA. For simplicity, we plot the log-

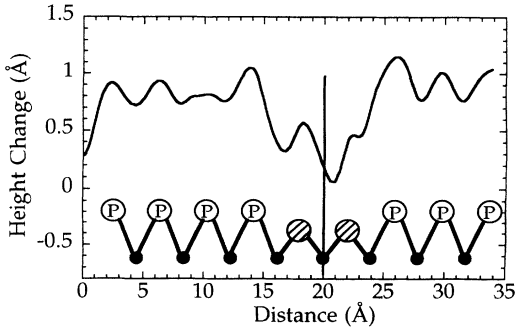

FIG. 5. Height profile measured across a strain-induced line defect, measured between the two arrows shown in the lower right of Fig. 2(b), and demonstrating the symmetry of defect with respect to the crystal lattice. Open circles are P atoms of P—P dimers; shaded circles are P atoms in the dimers which appear pulled into the surface in the STM images.

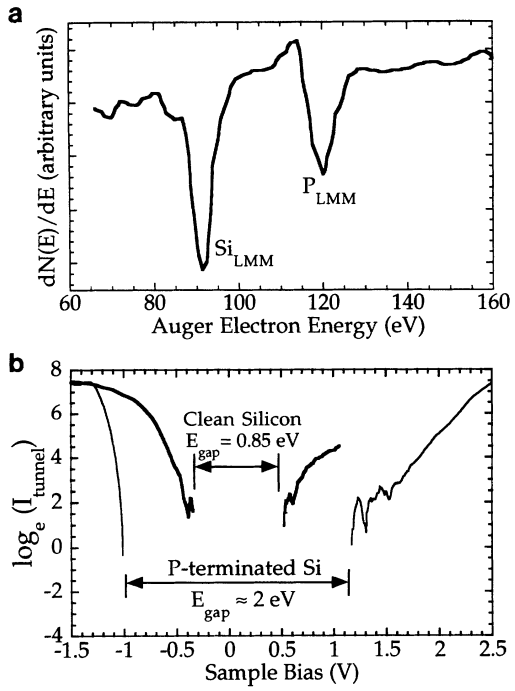

FIG. 6. (a) Auger-electron spectrum of the sample prepared as in Figs. 1–3, using 3 keV incident electron energy. (b) Tunneling spectroscopy data obtained on clean Si(001) surface (dark line) and on phosphorus-terminated surface (thin line), showing the increased band gap of the P-terminated surface.

arithm of the tunneling current vs sample voltage. On the clean surface, the data shows a gap approximately 0.85 eV wide, which is the energy difference between the occupied π and the unoccupied π^* antibonding levels of the clean Si=Si dimers; the gap is almost symmetrically distributed about the 0 V sample-tip bias, indicating that the Fermi level is pinned approximately midgap. These results are consistent with previous measurements of the clean Si(001) surface.[24] After formation of the P-terminated surface, Fig. 6(b) shows that the gap has broadened considerably, with the tunneling current rapidly plunging toward zero for negative voltages smaller than 1.0 V and for positive voltages smaller than about 1.2 V. The sharp increase in current near -1.1 V indicates a sharp increase in the surface density of states at 1.1 V below the Fermi energy. Based on the fact that the STM images reveal two well-resolved protrusions separated by 3.2 Å for the P—P dimers, we attribute this -1.1-eV electronic state to the lone-pair orbitals on the phosphorus atoms, as depicted in Fig. 4. Again, the tunneling characteristics are symmetrically distributed about zero sample-tip bias, indicating that although phosphorus substituting on a bulk Si lattice site acts as an n-type dopant, the Fermi energy for these phosphorus-passivated surfaces is still pinned approximately midgap.

B. Structure and properties of phosphorus overlayers below monolayer coverage

While at high coverage the surface consists primarily of P—P dimers and some Si—P dimers, these relative amounts of Si—P and Si=Si dimers will depend on the local phosphorus coverage. Figures 1–3 show that when the phosphorus coverage is slightly less than unity, the surface essentially consists of an alloy of P—P and Si—P dimers. In order to investigate this alloying in more detail, we conducted investigations of the surface structure with a lower coverage of phosphorus. These results show that reducing the phosphorus coverage significantly changes the surface morphology, the types of defects present, and the manner in which islands nucleate and grow on the surface.

Figures 7 and 8 show images at a successively higher resolution of a Si(001) surface which was prepared by exposing the Si(001) surface to only 1.5 L (a factor of 13 lower exposure than Figs. 1–3) PH_3 at 825 K. The large-scale STM image in Fig. 7(a) shows that there is still substantial silicon displacement, resulting in the formation of strongly anisotropic islands much like those in the earlier images. The amount of silicon displacement is substantially smaller, however, as in Fig. 7 it is quite easy to distinguish the original substrate from the islands produced by Si ejection, while in the earlier Figs. 1–3 it was

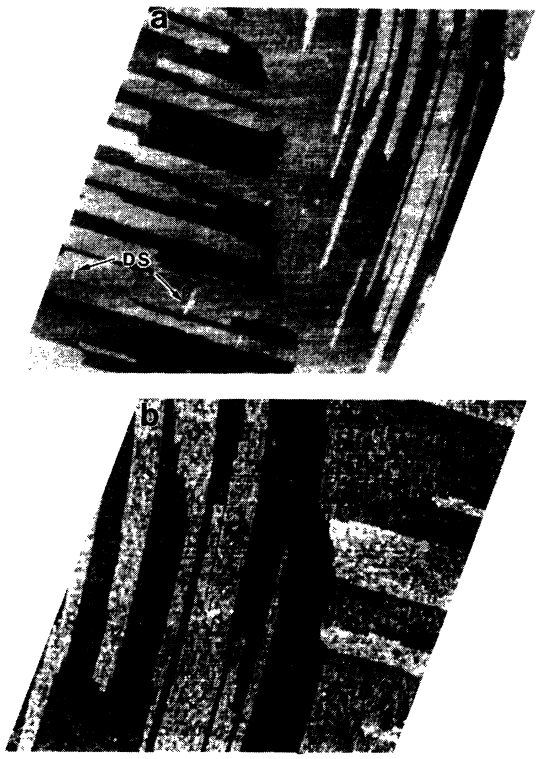

FIG. 7. (a) Large-scale STM image of surface partially covered by phosphorus, prepared as discussed in the text. Again note the formation of large anisotropic islands, but the absence of line defects. $V_{sample} = -2.15$ V, $I_{tunnel} = 0.2$ nA. Dimensions are 1250×1180 Å^2. (b) Higher-resolution STM image of partially P-terminated surface showing formation of highly anisotropic islands and the speckled appearance due to the mixture of Si=Si, Si—P, and P—P dimers. Note that the width of islands are no longer constrained by line defects. $V_{sample} = -2.15$ V, $I_{tunnel} = 0.2$ nA. Dimensions are 625×575 Å^2.

difficult to identify island and substrate terraces. A second, but less obvious difference from earlier images, is the complete absence of the line defects which were so pronounced at higher phosphorus coverage. Instead, the only line defects observed at this coverage are "AP1" and "AP2" antiphase boundaries formed (with 50% probability) when islands intersect.[23] The AP1 and AP2 boundaries can be observed in Figs. 7(a) and 7(b). The replacement of the LD with AP defects also changes the manner in which islands nucleate and grow on the surface. For example, in the lower left region of Fig. 7(a) there are several small dimer strings, indicated by "DS." Unlike at higher coverage where dimer strings nucleated adjacent to the line defects, in Fig. 7 each of these dimer strings has nucleated on an AP2 antiphase boundary, just like clean silicon. Thus, the nucleation and growth kinetics occurring on these surfaces appears to be more similar to that of clean silicon than to the P-terminated surface.

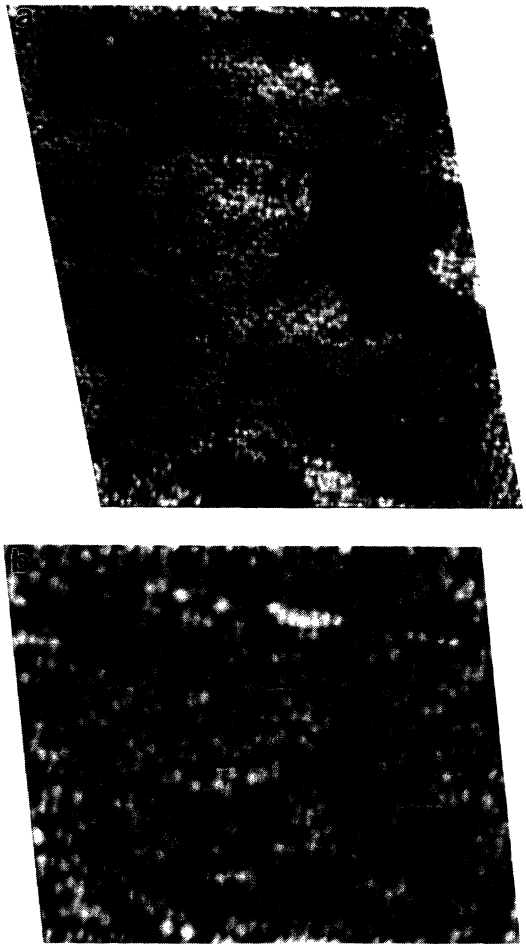

FIG. 8. (a) High-resolution STM image of partially P-terminated surface showing P—P and Si—P dimers; the chemical composition of the lower and upper terrace is the same. $V_{\text{sample}} = -2.2$ V, $I_{\text{tunnel}} = 0.2$ nA. Dimensions are 345×410 Å^2. (b) High-resolution image of partially P-terminated surface showing Si=Si, Si—P, and P—P dimers. Some Si=Si dimers are indicated with arrows; Si—P and P—P dimers can be found in numerous locations. There is a step edge near the top of the image. $V_{\text{sample}} = -2.2$ V, $I_{\text{tunnel}} = 0.2$ nA. Dimensions are 170×145 Å^2.

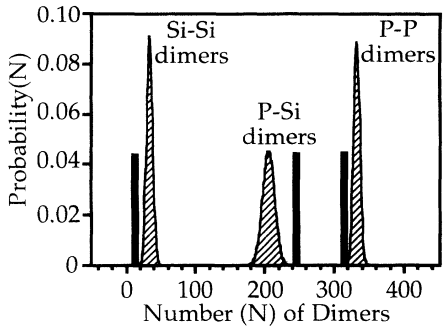

FIG. 9. Statistical analysis of the surface chemical composition obtained by counting the number of Si=Si, Si—P, and P—P dimers on the upper terrace of Fig. 8(b). Black bars indicate the experimental results, while the shaded graphs show the predicted probability distribution for a completely random alloy containing 866 P atoms and 270 Si atoms.

At higher resolution, Fig. 8(a) shows that the surface again takes on a mottled appearance due to the presence of silicon-phosphorus dimers. At the highest resolution, as in Fig. 8(b), it is possible to count the individual atoms. As in the earlier images, most of the white protrusions (Si atoms) are located to one side of the dimers, not on the center. However, at this lower P coverage some Si=Si dimers can be observed, giving rise to bean-shaped dimers just as on the clean surface. Two examples of Si=Si dimers are indicated by arrows in Fig. 8(b). In order to determine the surface stoichiometry and to investigate whether the spatial distribution of silicon and phosphorus in the surface layer is random, we counted the number of Si=Si, Si—P, and P—P dimers in images such as Fig. 8(b). On the upper terrace of Fig. 8(b) (the entire image except the topmost region), we counted 311 P—P dimers, 13 Si—Si dimers, and 244 Si—P dimers. For comparison, Fig. 9 shows the expected distribution functions for a surface containing 866 phosphorus atoms and 270 silicon atoms, paired randomly on a surface to form a random alloy of P—P, Si—P, and Si=Si dimers (shaded curves) compared with these experimental results (heavy vertical lines). The experimental results show that the distribution is not far from what would be expected based on pure statistics. However, there is a slight deviation which we believe to be real, resulting in a *larger* number of Si—P dimers and smaller numbers of Si=Si and P—P dimers than would be expected on the basis of pure statistics.

C. Partial overlayers produced by evaporation

To determine whether the observed surface structure is dominated by the growth kinetics, we also conducted experiments in which a completely phosphorus-terminated surface was heated to partially desorb phosphorus. Figure 10(a) shows a 8500×8500 Å region of a surface which was prepared by taking a surface which was com-

pletely passivated with P—P dimers, like those shown in Fig. 1, and subsequently annealing to 916 K for 60 s. The surface again shows formation of large islands and finger-like extensions and invaginations similar to those in previous figures. Auger-electron spectroscopy, as in Fig. 10(b), confirms that the surface phosphorus concentration is lower, giving a P/Si peak ratio of 0.23, approximately 40% of the peak ratio of 0.57 obtained for the samples used in Fig. 8. Note that due to the very short path length of electrons in the 70–100 eV range, however, the P/Si peak ratio may not be strictly proportional to concentration.

Higher-resolution images, such as Figs. 11(a) and 11(b), show that the surface again consists of a random alloy of silicon and phosphorus, but now with Si=Si dimers predominating. High-resolution images sometimes show small vacancy clusters in the outermost surface layer, as indicated by "V" in Fig. 11(a), which might be related to the desorption of phosphorus from the surface. Similarly to the medium-coverage regime, we find no evidence for line defects as strain reliefs, instead finding AP1 and AP2 boundaries which behave similarly to those observed in pure silicon epitaxy; for example, in the lower region of Fig. 11(a) we observe island nucleation on an AP2 domain boundary. Due to the presence of significant disorder in surfaces prepared in this way, we are unable to obtain reliable counting statistics of the number of dimers of each type. However, visual inspection of Fig. 11(b) shows the presence of significant numbers of Si=Si, Si—P, and some P—P dimers on this surface, indicating that the surface remains a nearly random alloy even when prepared by this method. Thus, we conclude that the alloying observed at higher coverages in Figs. 1–3 and 7–8 does not result from a kinetically limited process, but most likely describes the equilibrium distribution of Si=Si, Si—P, and P—P dimers. Just above center in Fig. 11(b) there does appear to be some preferential ordering of the P—Si dimers along a given dimer row, with a spacing of $2a_0$ between P—Si dimer units. This suggests some longer-range interactions between dimers which might be associated with dimer tilting (which typically alternates direction along a dimer row) or might arise from direct electrostatic interactions between Si—P dimers due to charge transfer from the P atoms to its Si dimer partner. Adsorbate-adsorbate interactions have been treated by Tang and Freeman for As and Sb adatoms on Si(001), but for a significantly different geometry.[25]

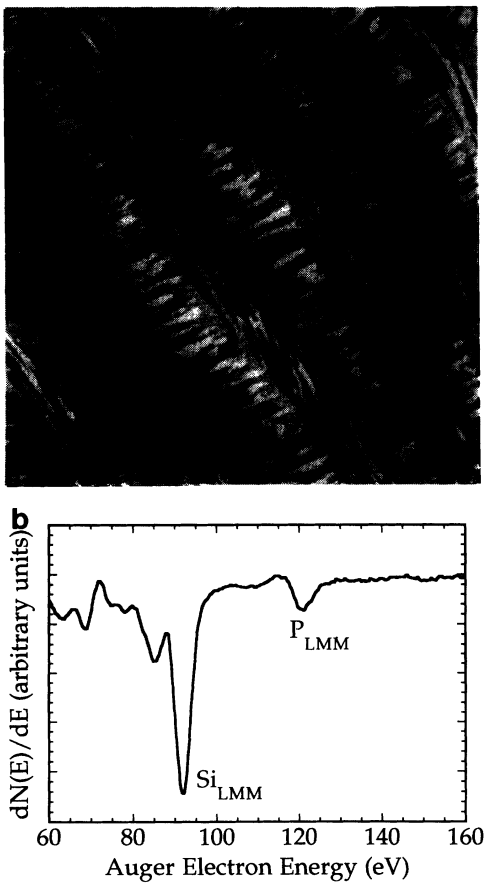

FIG. 10. (a) Large-scale STM image of Si(001) surface prepared by partial desorption of phosphorus from P-terminated surface $V_{sample}=-2.0$ V, $I_{tunnel}=0.1$ nA. Dimensions are 8500×8500 Å^2. (b) Auger-electron spectrum of surface shown in Fig. 8, showing that the P concentration is lower but still detectable.

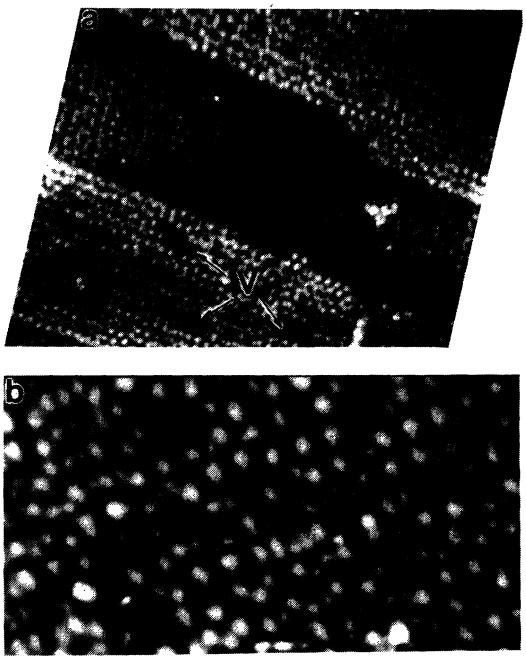

FIG. 11. (a) STM image of surface prepared by desorption of phosphorus from P-terminated surface showing formation of holes due to phosphorus evaporation. $V_{sample}=-2.0$ V, $I_{tunnel}=0.2$ nA. Dimensions are 341×261 Å^2. (b) High-resolution STM image of surface prepared by desorption of phosphorus from P-terminated surface showing P—P dimers, Si—P dimers, and Si—Si dimers. $V_{sample}=-2.0$ V, $I_{tunnel}=0.2$ nA. Dimensions are 126×261 Å^2.

IV. DISCUSSION

A. Geometric and electronic properties of P—P and Si—P dimers on Si(001)

Our results clearly show the formation of phosphorus-phosphorus and phosphorus-silicon dimers. The stability of the P—P dimers and their passivation of the surface can readily be understood based on their electronic structure. As a member of group V of the Periodic Table, phosphorus typically forms compounds in which the P atoms have a coordination number of 3, although compounds in which P has a coordination number of 5 are also possible. In a previous paper[26] investigating the room-temperature adsorption of PH_3 on Si(001), we found that the PH_3 molecule adsorbed directly on top of a Si=Si dimer, breaking the weak π bond of the dimer and instead forming two strong P—Si bonds, giving the P atom a coordination number of 5. At higher temperatures where the PH_3 dissociates and H desorbs from the surface, the phosphorus atom can substitute into the crystal lattice. Our present results show that this displacement reaction, in which a P atom adsorbed on top of the surface displaces Si from a Si=Si dimer and ejects it onto the surface, occurs at nearly random locations on the surface, since we find both phosphorus and silicon randomly distributed both on the islands and on the terraces. The final result is that the surface consists primarily of P—P and Si—P dimers.

We first consider the structure of the dimers. On the Si(001) surface, the (1×1) unit cell has dimensions of 3.84×3.84 Å^2. The normal Si=Si dimers are formally considered to have a double bond, due to the presence of a strong σ bond and a weak π bond; this bond formation results in a (2×1) unit cell in which the two Si atoms within a dimer are separated by 2.30 Å.[27] Interaction with chemical species such as hydrogen occurs by breaking the weak π bond, leading the σ bond intact, and forming two new bonds to the adsorbate; because the strong σ bond remains intact, the Si—Si dimer bond lengthens only slightly, to 2.51 Å.[28]

Phosphorus typically forms chemical compounds through sp^3 hybridization, such that the three bonds are formed at three legs of a tetrahedron, with the fourth leg occupied by the "lone pair" electrons, similar to the ammonia molecule. In the compound P_2H_4, for example, the P atoms are bonded to one another with a bond distance of 2.11 Å (Ref. 29) and the hydrogen atoms found in a "gauche" configuration (on the same side of a mirror plane containing the P—P bond). Replacing the four hydrogen atoms of this molecule with four Si atoms of the bulk-terminated Si(001) surface produces a dimerized, P_2-terminated surface. A number of other phosphorus compounds of this general shape are found, including P_2H_4 ($R_{PP}=2.11$ Å),[29] PF_2PH_2 ($R_{PP}=2.22$ Å),[30] P_2I_4 ($R_{PP}=2.21$ Å),[31] and $P_2(CH_3)_4$ ($R_{PP}=2.19$ Å),[32] all of which show P—P bond lengths comparable to the value of 2.21 Å observed for P_4 vapor.[33] While in the solid phase only P_2H_4 adopts the gauche configuration and all others adopt a trans configuration to minimize steric repulsion between the substitutent groups, studies show that the rotational barrier between the trans and gauche configurations is small.[31,32] Thus, we expect that a P—P dimer on Si(001) will involve a P—P bond distance of approximately 2.2 Å, which is slightly shorter than the 2.30-Å dimer bond length of the clean Si(001) surface. Likewise, Si—P bond lengths can be estimated from data on the compounds $H_3Si—PH_2$ and $(H_3Si)_3P$, in which the Si—P bond lengths are 2.249 and 2.248 Å, respectively.[34] These Si—P bond lengths are again slightly smaller than the Si—Si bond lengths in the bulk (2.35 Å) and also shorter than the 2.41-Å bond length between a dimerized Si atom and the underlying Si surface determined by Chabal and Raghavachari[28] for the Si(001)-(2×1)H monohydride surface. Since both the P—P dimer bond and the P—Si dimer-substrate bond are shorter than the corresponding bond lengths for silicon dimers, we expect that the phosphorus-terminated surface is in *tensile* stress relative to clean Si(001)-(2×1). For comparison, the As—As dimer bond length in As-terminated Si(001) is 2.55 Å,[27] considerably longer than the Si=Si dimer bond length and just slightly longer than the length of a single Si—Si dimer bond, measured at 2.51 Å for the Si(001)-(2×1)H monohydride structure.[28]

In addition to the role of bond lengths in surface energetics, Meade and Vanderbilt[35] have emphasized the contributions of bond angle strain. Electrons in lone pair orbitals give rise to larger Coulombic repulsion terms than those in chemical bonds, so that the P atoms in P—P dimers should deviate from tetrahedral coordination in such a way as to decrease the Si—P—Si bond angle. However, this bond angle can only be decreased by a concommitant *increase* in the Si—P bond distance compared with Si—Si. The net result is that compared with the Si—Si dimer, the P—P dimer has strain induced by both the shorter bond distance and the strained bond angles, which reinforce one another and lead to a high energy for P—P dimers.

The electronic properties of these P—P dimers can be understood based on the fact that the Si—P and P—P bonds are quite strong and likely involve a strong separation between the appropriate highest occupied and lowest unoccupied orbitals, i.e., there is a large bandgap. In STM studies of clean silicon surfaces, images obtained at positive and negative bias appear quite different[19,24] because electron tunneling occurs through the occupied π and unoccupied π^* surface states, which lie relatively close to the Fermi energy. In the case of the P—P dimers, the gap is considerably larger. At negative bias, electrons most likely tunnel out of the lone pair orbitals on the P atoms, which our tunneling spectroscopy results indicate lies at 1.1 eV below the Fermi energy. This is supported by the line profile measurements in Fig. 3, which show that the separation between maxima in the STM images is 3.2 Å, significantly larger than the 2.2-Å separation between P atoms and near the location where one would expect the lone pair orbitals to be. At positive bias, we noted earlier that it is difficult to achieve tunneling and the resulting images show very little contrast for P—P dimers. Likewise, the tunneling spectroscopy data in Fig. 6 indicate that the current at positive bias increases quite slowly with increasing voltage compared

with that at negative voltage and does not show a sharp "turn-on" at a characteristic voltage. We attribute the lack of spatial and electronic contrast at positive voltages to the absence of any P-derived unoccupied energy levels; instead, electrons likely tunnel directly into the conduction band and, therefore, show no atomic contrast. This interpretation is consistent with that used by Becker, Klitsner, and Vickers,[13] who found a similarly large bandgap for As—As dimers on Si(001), with an occupied state near -1.6 V attributed to the arsenic lone-pair and an unoccupied state near $+1.4$ V attributed to an As—Si backbond. They also found only weak contrast at positive sample voltages.

Although at first the formation of a P—Si dimer with an unsaturated dangling bond might be considered unfavorable, our results clearly show that this is not true. If we consider the disproportionation reaction $2(\text{P—Si}) \rightarrow \text{Si}=\text{Si}+\text{P—P}$, substituting in the results of our counting measurements produces an equilibrium constant K_{eq} of 0.07. If we use the thermodynamic relationship $\Delta G = -RT\ln(K_{eq})$ where R is the universal gas constant (8.31 $\text{J mol}^{-1}\text{K}^{-1}$) and T is absolute temperature, and if we assume that the equilibrium is "frozen in" at a temperature which we arbitrarily assume to be 500 K, this implies a free-energy change of approximately 11 kJ/mole or 0.1 eV per dimer (0.05 eV per P—Si dimer). Thus, our measurements indicate that the P—Si bond is 0.05 eV *more* stable than the average energy of a Si=Si dimer and a P—P dimer. While more detailed counting statistics are needed to obtain accurate equilibrium constant values, the data above clearly show that it is not energetically unfavorable to form a P—Si dimer, and it might even be energetically favorable.

In the case of a P—Si dimer, the phosphorus atom is again able to achieve a favorable bonding configuration, but the silicon atom is left with a total of three bonds and a fourth dangling bond. Because this dangling bond is only partially occupied, electrons can readily tunnel out of these Si atoms at negative sample bias and into these Si atoms at positive sample bias. As a result, these Si atoms appear as protrusions both at negative and positive sample bias, in agreement with our experimental observations. Recent theoretical investigations by Yu and Oshiyama[15] have predicted the existence of a stable Si—As heterodimer and have suggested that such heterodimers may play an important intermediate in the substitutional As doping. Their electronic-structure calculations for Si—As dimers are also quite consistent with what we observe for Si—P dimers—at negative sample bias (filled states) and voltages of less than 1 V, they predicted that the STM images would reveal a protrusion over the location of the Si atom. While they also predicted that at larger negative voltages the contrast would reverse and the As atom would appear higher, we have not observed a contrast reversal in the Si—P system. We expect that Si—P heterodimers might be stabilized by electron transfer from the phosphorus lone pair to the Si dangling bond and might also be stabilized by tilting of the dimer; dimer tilting could help reduce the Si—P bond distance and optimize the bond angles around both Si and P atoms.[35] Indeed, on Si(001) both theoretical[36,37] and experimental[21] results show that tilting and charge transfer are related, since tilting a Si=Si dimer transfers electron density from the lower atom to the upper atom. Because the STM images contain a mixture of geometric and electronic contrast, we are not able to establish with certainty whether Si—P dimers are tilted or not. However, we note that in the case of Si=Si dimers, it is often observed that when the mirror plane bisecting the Si=Si dimers bond is broken (such as by a point defect or step edge) causing one dimer to tilt, the titling of one dimer usually induces a tilting in its adjacent neighbor in the opposite direction, ultimately producing a zig-zag chain of alternately tilting dimers which propagates 10–15 Å along the dimer row away from the initial site.[18,20] Close inspection of the images in Figs. 3(a) and 8(b) shows that the P—P dimers adjacent to P—Si dimers do *not* appear to be buckled; this indicates that either (static) tilting of Si—P dimers is small, or else that surface P—P dimers do not respond in the same way as Si=Si dimers of the clean surface.

The formation of large numbers of silicon dangling bonds upon phosphorus adsorption is also consistent with a previous study by Yu and co-workers,[16,17] who used photoemission spectroscopy to study the energy of the bulk silicon $2p$ state as a function of phosphorus coverage. They found that the Si $2p$ state remained constant in energy until the phosphorus coverage reached a critical value close to one full monolayer. At near monolayer coverage, the $2p$ state rapidly increased in binding energy by 0.45 eV, indicating that the surface becomes unpinned and the near-surface region becomes doped n type with the Fermi level near the conduction band. They interpreted this pinning effect as arising from charge transfer to a band of intrinsic unoccupied surface states (the π^* antibond band) of the clean Si=Si dimers. However, our results show that it more likely arises from the large number of Si dangling bonds created by the formation of P—Si dimers. Since at coverages below 0.5 monolayer there is approximately one dangling bond created for each phosphorus atom, it is only at high coverages, where the number of P—P dimers overwhelms the number of Si—P dimers, that doping can be achieved in the near-surface region.

B. Surface morphology and defect structure

As noted above, one distinguishing feature between the images obtained at high P coverage (near 1 monolayer) and those obtained at lower coverage is that at high coverage, the surface contains a large number of line defects which cut perpendicular to the dimer rows. In a previous study of phosphorus on Si(001) using low-energy electron diffraction, Yu and co-workers[5,16,17] found that the (2×1) reconstruction was retained upon formation of a phosphorus overlayer, but the LEED pattern showed strong streaking. Our images suggest that the streaks most likely arise from the line defects and the extensive islanding which occurs within the LEED electron coherence length of approximately 100 Å.

Line defects on Si(001) have been observed under several circumstances. Niehus *et al.*[38] showed that

transition-metal contamination creates line defects similar to those observed in Figs. 1–3, giving rise to $(2\times n)$ reconstructions where n can vary between approximately 8 and 12 depending on the amount of Ni contamination; the defect formation was attributed to a strain effects arising from subsurface nickel.[38] We rule out such contamination effects here based on the fact that the line defects observed in Figs. 1 and 2 disappear when the phosphorus is desorbed from the surface by heating to 1400 K, while transition-metal contamination is usually impossible to remove by such treatments.

A second class of line defects can also be created when islands exhibiting a (2×1) reconstruction intersect, with a translational shift of 3.84 Å ($=a_0$) between the islands perpendicular to the dimer row. Such "antiphase" boundaries can occur in two ways: antiphase boundaries in which the dimer rows meet "head on" but shifted by 3.85 Å are denoted "AP2" boundaries, while antiphase boundaries in which the dimer rows meet side by side are denoted "AP1." In silicon homoepitaxy at low temperatures, Bronikowski, *et al.* showed that Si island nucleation occurs almost exclusively by first covering up AP2 boundaries to form one-dimensional dimer strings, and subsequently expanding to form elongated Si islands, effectively burying the AP2 boundary.[23] However, the line defects visible in Figs. 1–3 behave quite differently than those observed on the clean Si surface. First, we note that on clean silicon, dimer rows which meet head on simply fill in to form a complete overlayer, and the boundary between them disappears. In contrast, Fig. 2 shows that for the phosphorus overlayer the line defects produced when dimer rows intersect head on but out of phase by one lattice constant, but also when the dimer rows intersect without any lateral phase difference—that is, the line defects observed for the phosphorus overlayers do not arise simply from the intersection of islands which have out-of-phase (2×1) reconstruction, but they instead appear to be intrinsic to the phosphorus-overlayer surface. Also, whereas for pure silicon epitaxy the dimers nucleate efficiently directly on top of the AP2 boundaries, for phosphorus overlayers the islands nucleate *adjacent* to the boundary but actually avoid crossing the boundary itself, as can be clearly observed in Figs. 1 and 2. Thus, it is clear that the line defects observed here are not the antiphase boundaries observed earlier for silicon homoepitaxy. Instead, we believe the line defects in Figs. 1–3 are a strain-relief mechanism resulting from the fact that the Si=Si dimer bond length is substantially different from the P—P dimer bond length, inducing strain in the underlying crystal lattice. Line defects consisting of vacancies then act as a strain-relief mechanism.

The formation of defects as a strain-relief mechanism has been proposed previously for several systems. For silicon, it has been proposed that ordered "$2\times n$" structures on Si(001) arise from ordered arrays from defects,[38–41] which are present either to remove intrinsic strain or in response to strain fields created by subsurface contamination by transition metals or other impurities. More recently, investigations of germanium deposition on silicon have shown that the 4.3% lattice mismatch between Si and Ge also results in the formation of line defects that cut perpendicular to the Ge dimer rows and with a spacing varying with the Ge coverage.[10,11,42] Tersoff has recently shown that vacancy defects, originally proposed by Pandey,[39] believe the compressive strain induced by Ge adsorption by allowing dimerization of second-layer atoms in a direction perpendicular to that of the top-layer atoms. This so-called "π-bonded defect" is also believed to account for many of the missing dimer defects observed on clean Si(001) surfaces.[18,20]

Based on simple symmetry arguments, we can state unequivocally that the line defects observed in the case of phosphorus overlayers cannot be the π-bonded defect originally proposed by Pandey[39] and recently studied by Tersoff.[12] The STM images in Figs. 2 and 3 and the line scan in Fig. 5 show that the line defects appear like two dimers which are pulled into the surface, with a slight gap between them which looks at first like a dimer vacancy. The line profile in Fig. 5 clearly shows that the total width of the line defect, including both "pulled-in" dimers, is $2a_0$, where $a_0=3.84$ Å is the spacing between dimers along a dimer row. As a result, the center of this defect lies midway between two surface dimers and directly over a second-layer atom, while in the π-bonded defect model the center of the defect lies midway between second-layer atoms. Therefore, symmetry arguments alone rule out the π-bonded defect model as the origin of these trenches. This is further supported by calculations of the strain field produced by π-bonded defects. Tersoff[12] and Pandey[39] have shown that along a dimer row (which for a Ge overlayer on Si is in compressive stress), the presence of a π-bonded defect lowers the energy by adding tensile stress, thereby reducing the total stress. For phosphorus overlayers, however, we noted above that we expect all bond lengths to be shorter than for the Si=Si dimers, which means that formation of a phosphorus-terminated surface places the surface in *tensile* stress. In that case, adding π-bonded defects would increase both the total stress and the total surface energy. If the major reason for forming defects is to act as a strain relief, then on the P-terminated surface we expect that such defects need to add *compressive* stress in order to stabilize the surface.

The STM images alone cannot unambiguously determine the structure of these defects because there are several possible models having the correct symmetry. Figure 12 schematically shows the symmetry of the line defects in top and side views. The STM images suggest that the dimers which appear to be pulled in toward the surface are indeed present, and the fact that these defects are observed only at the highest P coverages suggests that they are most likely P—P dimers; these dimers are labeled "1" in Fig. 12. The line scan in Fig. 5 as well as visual inspection of Figs. 2(b) and 3(a) shows that the defect must have a total width of $2a_0$, with the center of the defect midway between two dimers and directly above a second-layer atom as indicated by the dotted line in Fig. 12. Likewise, the line defects do not induce any dimer tilting, suggesting that the line defects preserve the mirror plane running along the center of the dimer rows bisecting the P—P dimer bonds. There are many ways of creating line defects consistent with these observations,

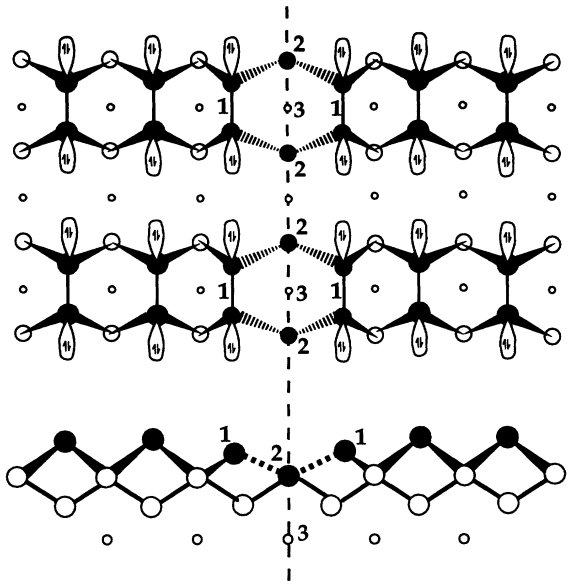

FIG. 12. Schematic model for line defects. The dotted line indicates the mirror symmetry plane observed in the STM images. Numbered atoms are described in the text.

but the evidence suggests that the most likely possibilities involve either substitution of P for Si or else creation of a vacancy. We note that Yu, Vitkavage, and Meyerson[17] found that exposure of Si(001) to PH_3 only produced a Fermi-level shift at very high P coverages, where P—P dimers predominate and the line defects appear. While we attributed the absence of any measurable doping effect to the presence of large numbers of dangling bonds on Si—P heterodimers at intermediate coverages, it is also possible that P atoms do not efficiently enter substitutional locations until very high coverage where P—P dimers predominate, and, therefore, the line defects my arise form the presence of P atoms in subsurface substitutional sites. In order to maintain the overall symmetry evident in the STM images, the creation of a vacancy or a substitution must occur either at all the atoms labeled "2" (and depicted in black in Fig. 12), or else at the atoms labeled "3." More complex defects structures are also possible, and further work will be required to determine the atomic configuration more definitively.

The line defects appear to be affected by at least two variables: the chemical composition of the surface (P/Si ratio), and the local surface morphology. The influence of chemical composition is quite strong, as images near monolayer phosphorus coverage (as in Figs. 1–3) show large numbers of line defects, while images at lower concentration (as in Figs. 7 and 8) do not show line defects at all. Thus, the density of line defects appears to be a strong, nonlinear function of the surface phosphorus coverage.

As previously pointed out by Tromp and coworkers[8,9,11] and Tersoff,[12] in a simple strain-relief model for a binary system (such as Ge on Si, without allowing for Ge—Si heterodimers), the number density of strain-relieving defects should increase smoothly as the adlayer coverage is increased. In the case of Ge/Si, for example, strain-relieving defects have a spacing of $12a_0$ at 1 monolayer coverage, decreasing to $8a_0$ at 2 monolayer.[10,11] Applying this idea to the case of arsenic adsorption, where As—As dimers form an adsorbed layer on top of the Si substrate under some conditions but displace silicon from the outermost layer to form As—As dimers in the surface plane (with silicon adatoms presumably diffusing to step edges), Tromp showed that if the surface energy vs coverage curve is nonlinear, it can become favorable to have displacive adsorption at intermediate coverages, while if the curve is linear the system will tend to have regions of adsorbed As—As dimers atop the silicon surface coexisting with the substrate containing Si=Si dimers. In this and most other models of surfactant growth and interfacial stress, however, it has been assumed that the surface structure consists of a two-phase system, such as As—As dimers and Si—Si dimers, for example, and that heterodimers such as As—Si dimers are not present.

In the Si—P case, our experiments lead us to conclude that the formation of heterodimers such as Si—P can play a significant role in the surface energetics. Our experiments indicate that while P—P dimers add significant tensile stress to the surface (therefore, causing line defects), Si—P dimers do not. For a random statistical alloy of Si=Si, P—P, and Si—P dimers, we would expect the fraction of the surface occupied by P—P dimers to increase as Θ^2, where Θ is the fractional surface coverage of phosphorus. If we assume that the surface stress is primarily due to the P—P dimers, then the surface stress also increases like Θ^2. In this case, the density of line defects is small (or zero) at small and intermediate P coverages, but rapidly increases in number as the P coverage approaches unity, in agreement with experiments. We also note that our counting statistics show that the free-energy change associated with the disproportionation reaction 2(P—Si)→Si=Si+P—P is slightly positive, leading to preferential formation of P—Si dimers at the expense of Si=Si and P—P dimers. The (slightly) nonstatistical distribution of Si=Si, Si—P, and P—P dimers might arise at least partially from the strain associated with formation of P—P dimers.

Even for a surface with a given chemical composition, Figs. 1 and 2 show that the spacing between line defects is variable. However, there is a consistent trend: the line defects are always close together on extended terraces and are farther apart on narrow islands and "fingers" extending from larger terraces. Rough counting statistics indicate that the chemical composition of the surface is uniform, so the variation in spacing is likely related to the island morphology, rather than its chemical composition. Taking Fig. 2(a) as an example, measurement of the spacing between line defects on the islands yields an average spacing of $14a_0$, while on the lower terrace it is $6a_0$. Yet, the chemical composition of these terraces is essentially the same. The few residual Si—P dimers can be easily identified (and counted) based on the density of white protrusions in the image, which is essentially identical on the two terraces. Likewise, the lower left region of Fig. 1 shows many fingers, with an average spacing of

about $14a_0-16a_0$, extending from a terrace with a larger number of line defects separated by about $6a_0-8a_0$. We believe that the variable line number might arise from stress buildup parallel to the dimer bond direction, which is easily relieved in the smaller dimer islands and finger-like projections due to their narrow width, but on larger terraces produces a higher density of line defects. This increase in line defect density on flat terraces compared with narrow, long islands thus suggests that the defects reduce the overall stress tensor both parallel to the dimer rows and perpendicular rows, resulting in a large decrease in the overall surface free energy.

In addition to acting as a strain relief and thereby changing the total surface energy, the line defects in Figs. 1–3 also play a role in the growth kinetics by affecting both the island nucleation and growth. Figures 1–3 show that island nucleation occurs adjacent to these defects, first forming one dimensional dimer strings parallel to the defect. We note that unlike epitaxy on Si(001), where islands nucleate on antiphase defects and quickly cover up the defect, for the phosphorus overlayers just the opposite is true. The islands nucleate adjacent to line defects, but the growing islands tend to be constrained by the line defects; where the line defects are dense, as in the Fig. 1(b) (line defects visible at lower left and upper right) and in Fig. 2(b), the islands become very long and narrow. Because growth occurs at elevated temperatures where the line defects might also be mobile, it is also possible that nucleation occurs randomly and that these islands, once formed, pin the location of the line defects. Irrespective of the exact mechanism, the STM images reveal that further growth occurs in both dimensions but producing very anisotropic islands. In general, the islands appear to be more anisotropic than islands produced by epitaxial growth of silicon or germanium on Si(001). Both for Si homoepitaxy[22,43] and for Ge/Si heteroepitaxy,[42,44–46] anisotropic islands arise from a combination of two effects. First, the effective "sticking coefficient" for adatoms approaching the type "A" step edge (which runs parallel to the dimer rows of the islands) is much smaller than the sticking coefficient for adatom approaching the type "B" step edge (which cuts perpendicular to the dimer rows).[34] As a result, the islands tend to grow faster parallel to the dimer rows, resulting in long, narrow islands. Additionally, there is a thermodynamic contribution due to the different energies of the A and B step edges;[22,47] the equilibrium island shape is, therefore, also anisotropic, with an aspect ratio estimated[43] at approximately 3:1. In the P/Si system, we have in addition to these factors the additional contributions from the one-dimensional shape of the initial nuclei and the "bounding" action of the line defects. Thus, the overall anisotropy can be attributed to a combination of four factors: (1) the nucleation process, which forms dimer "strings" along the line defects (at high coverage) or at antiphase boundaries (at low coverage), (2) line defects in the underlying substrate layer, which appear to constrain the islands, (3) anisotropies in the sticking coefficients for diffusing atoms which react the two inequivalent types of step edges, and (4) thermodynamic asymmetry resulting from the different energies of the two inequivalent step edges. Further work will be required to determine the relative importance of these factors.

V. CONCLUSIONS

Exposure of Si(001) surfaces to PH_3 at elevated temperatures dramatically changes the morphology and chemical properties of the surface through the formation of P—P dimers and Si—P dimers. At full monolayer coverage, STM images show the formation of P—P dimers. Tunneling spectroscopy measurements show that these dimers have a very low density of states near the Fermi energy, which in turn results in a low chemical reactivity and likely accounts for the passivation of Si surfaces in CVD processes that use PH_3 as a dopant precursor. However, the effect of phosphorus is more complex than simple passivation, since the surfaces also reveal drastic changes in morphology, with the formation of large numbers of islands on previously flat terraces and the extreme roughening of step edges. Line defects are visible on the surface at saturation coverage, but the symmetry of the STM images shows that they cannot be the π-bonded defects that were earlier proposed by Tersoff as a strain relief for Ge growth on Si(001); we attribute the difference to the fact that phosphorus overlayers likely place the surface in tensile stress while Ge places the surface in compressive stress. These line defects also influence the growth kinetics and the ultimate growth morphology both by serving as nucleation sites for island growth and by bounding the lateral extent.

At less than monolayer phosphorus coverage, STM images reveal that the line defects disappear and the surface consists of a large number of Si—P dimers coexisting with the P—P dimers. Counting statistics indicate that the surface can be described as a nearly random alloy of P—P, Si=Si, and Si—P dimers but with a small nonstatistical preference for formation of Si—P heterodimers. The chemical makeup of the surface appears to strongly influence the growth kinetics; on the surfaces composed predominantly of Si—P dimers the morphology, nucleation, and growth processes are similar to clean Si, while near monolayer coverage the surface adopts clearly distinct morphology and shows quite different nucleation and growth behavior. Although the formation of heterodimers has not been widely considered previously, our results suggest that such heterodimers might play an important role in strain relief in overlayer systems and are a likely intermediate in dopant incorporation into the silicon bulk during CVD growth.

ACKNOWLEDGMENTS

This work was supported in part by the U.S. Office of Naval Research Solid State and Surface Chemistry Program and the National Science Foundation.

*Author to whom correspondence should be addressed. Electronic address: HAMERS@BERT.CHEM.WISC.EDU

[1]R. F. C. Farrow, J. Electrochem. Soc. **121**, 899 (1974).
[2]F. Eversteyn and B. H. Put, J. Electrochem. Soc. **120**, 106 (1973).
[3]C. A. Chang, J. Electrochem. Soc. **123**, 1245 (1976).
[4]B. S. Meyerson and W. Olbricht, J. Electrochem. Soc. **131**, 2361 (1984).
[5]B. S. Meyerson and M. L. Yu, J. Electrochem. Soc. **131**, 2366 (1984).
[6]M. Copel *et al.*, Phys. Rev. Lett. **63**, 632 (1989).
[7]M. Copel *et al.*, Phys. Rev. B **42**, 11 682 (1990).
[8]R. M. Tromp and M. C. Reuter, Phys. Rev. Lett. **68**, 954 (1992).
[9]R. M. Tromp, A. w. Denier van der Gon, and M. C. Reuter, Phys. Rev. Lett. **68**, 2313 (1992).
[10]R. M. Tromp and M. C. Reuter, Phys. Rev. Lett. **68**, 954 (1992).
[11]R. M. Tromp, Phys. Rev. B **47**, 7125 (1993).
[12]J. Tersoff, Phys. Rev. B **45**, 8833 (1992).
[13]R. S. Becker, T. Klitsner, and J. S. Vickers, J. Microscopy **152**, 157 (1988).
[14]R. D. Bringans, D. K. Biegelsen, and L.-E. Swartz, Phys. Rev. B **44**, 3054 (1991).
[15]B. D. Yu and A. Oshiyama, Phys. Rev. Lett. **71**, 585 (1993).
[16]M. L. Yu and B. S. Meyerson, J. Vac. Sci. Technol. A **2**, 446 (1984).
[17]M. L. Yu, D. J. Vitkavage, and B. S. Meyerson, J. Appl. Phys. **59**, 4032 (1986).
[18]R. J. Hamers, R. M. Tromp, and J. E. Demuth, Phys. Rev. B **34**, 5343 (1986).
[19]R. J. Hamers, R. M. Tromp, and J. E. Demuth, Surf. Sci. **181**, 246 (1987).
[20]R. J. Hamers and U. K. Köhler, J. Vac. Sci. Technol. A **7**, 2854 (1989).
[21]R. J. Hamers, R. M. Tromp, and J. E. Demuth, Phys. Rev. Lett. **56**, 1972 (1986).
[22]R. J. Hamers, U. K. Kohler, and J. E. Demuth, Ultramicroscopy **31**, 10 (1989).
[23]M. J. Bronikowski, Y. Wang, and R. J. Hamers, Phys. Rev. B **48**, 12 361 (1993).
[24]R. J. Hamers, P. Avouris, and F. Bozso, Phys. Rev. Lett. **59**, 2071 (1987).
[25]S. Tang and A. J. Freeman, Phys. Rev. B **48**, 8068 (1993).
[26]Y. Wang, M. J. Bronikowski, and R. J. Hamers, J. Phys. Chem. **98**, 5966 (1994).
[27]N. Jedrecy *et al.*, Surf. Sci. **230**, 197 (1990).
[28]Y. J. Chabal and K. Raghavachari, Phys. Rev. Lett. **53**, 282 (1984).
[29]M. Baudler and L. Schmidt, Z. Anorg. Allg. Chem. **289**, 219 (1957).
[30]R. L. Kuczkowski, H. W. Schiller, and R. W. Rudolph, Inorg. Chem. **10**, 2505 (1971).
[31]Y. C. Leung and J. Waser, J. Phys. Chem. **60**, 539 (1956).
[32]A. McAdam, B. Beagley, and T. G. Hewitt, Trans. Faraday Soc. **66**, 2842 (1970).
[33]L. R. Maxwell, S. B. Hendricks, and V. M. Mosley, J. Chem. Phys. **3**, 699 (1935).
[34]H.-G. Horn, Chemiker-Zeitung **110**, 131 (1986).
[35]R. J. Meade and D. Vanderbilt, Phys. Rev. Lett. **63**, 1404 (1989).
[36]D. J. Chadi, Phys. Rev. Lett. **43**, 43 (1979).
[37]G. P. Kerker, S. G. Louie, and M. L. Cohen, Phys. Rev. B **17**, 706 (1978).
[38]H. Niehus *et al.*, J. Microscopy **152**, 735 (1988).
[39]K. C. Pandey, *Pi-bonded Defect Model for Si(001),* Proceedings of the Seventeenth International Conference on the Physics of Semiconductors, edited by J. D. Chadi and W. J. Harrison (Springer-Verlag, New York, 1985).
[40]J. A. Martin *et al.*, Phys. Rev. Lett. **56**, 1936 (1986).
[41]T. Aruga, H. Tochihara, and Y. Murata, Phys. Rev. B **34**, 8237 (1986).
[42]U. Kohler *et al.*, Ultramicroscopy **42-44**, 832 (1992).
[43]Y.-W. Mo *et al.*, Phys. Rev. Lett. **63**, 2393 (1989).
[44]Y.-W. Mo and M. G. Lagally, J. Cryst. Growth **11**, 876 (1991).
[45]F. Iwawaki, M. Tomitori, and O. Nishikowa, Ultramicroscopy **42-44**, 902 (1992).
[46]Y. W. Mo and M. G. Lagally, Surf. Sci. **248**, 313 (1991).
[47]J. D. Chadi, Phys. Rev. Lett. **59**, 1691 (1987).

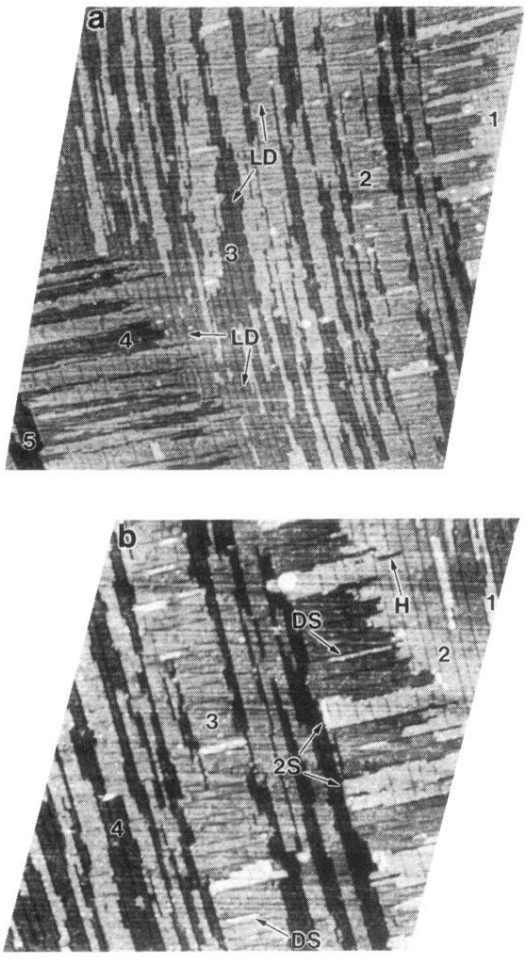

FIG. 1. (a) Large-scale STM image of phosphorus-terminated Si(001) surface, showing spontaneous island formation and the presence of line defects cutting perpendicular to the dimer rows. "1" denotes highest terrace, "5" the lowest. $V_{\text{sample}} = -2.0$ V, $I_{\text{tunnel}} = 0.2$ nA, Dimensions are 1150×1200 Å^2. (b) STM image of P-terminated Si(001) surface. Note the dimer string (DS) nucleated adjacent to a line defect and other islands at upper right bounded on their long sides by line defects. "1" denotes the highest terrace, "4" the lowest. "2*S*" denotes double-height step. $V_{\text{sample}} = -2.0$ V, $I_{\text{tunnel}} = 0.2$ nA; Dimensions are 675×710 Å^2.

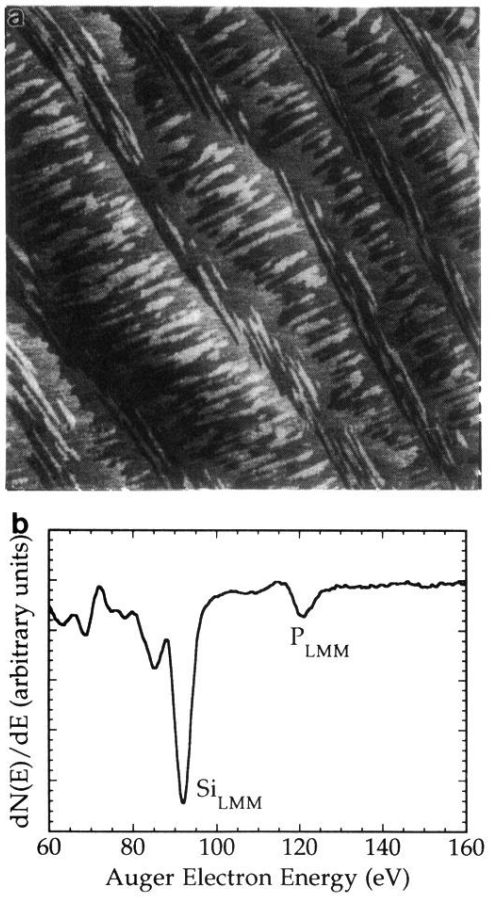

FIG. 10. (a) Large-scale STM image of Si(001) surface prepared by partial desorption of phosphorus from P-terminated surface $V_{\text{sample}} = -2.0$ V, $I_{\text{tunnel}} = 0.1$ nA. Dimensions are 8500×8500 Å^2. (b) Auger-electron spectrum of surface shown in Fig. 8, showing that the P concentration is lower but still detectable.

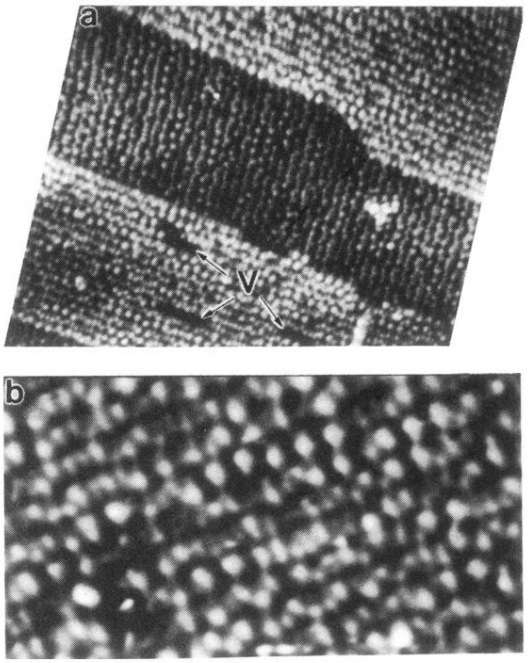

FIG. 11. (a) STM image of surface prepared by desorption of phosphorus from P-terminated surface showing formation of holes due to phosphorus evaporation. $V_{\text{sample}} = -2.0$ V, $I_{\text{tunnel}} = 0.2$ nA. Dimensions are 341×261 Å^2. (b) High-resolution STM image of surface prepared by desorption of phosphorus from P-terminated surface showing P—P dimers, Si—P dimers, and Si—Si dimers. $V_{\text{sample}} = -2.0$ V, $I_{\text{tunnel}} = 0.2$ nA. Dimensions are 126×261 Å^2.

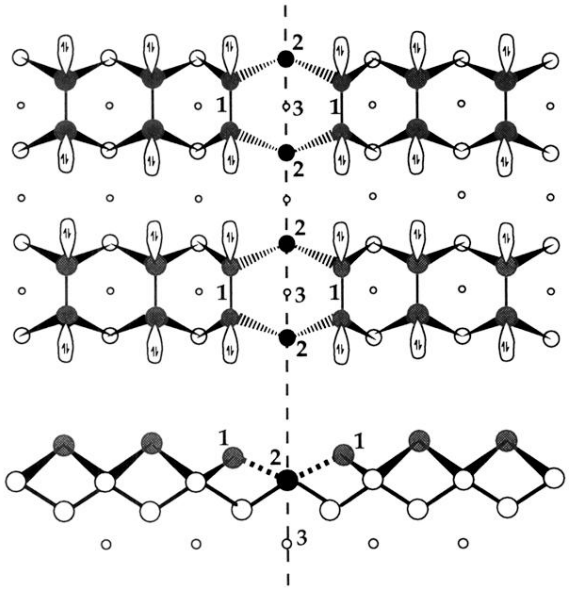

FIG. 12. Schematic model for line defects. The dotted line indicates the mirror symmetry plane observed in the STM images. Numbered atoms are described in the text.

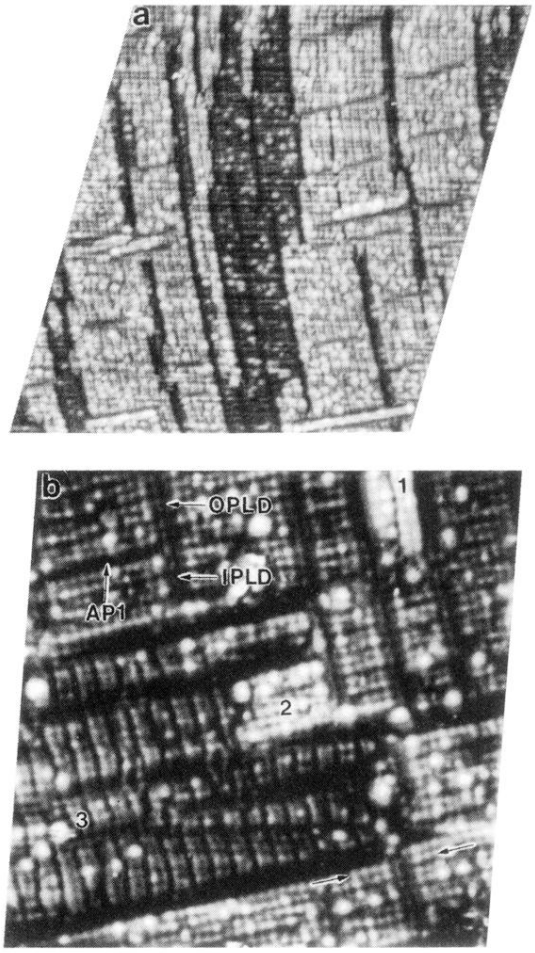

FIG. 2. (a) High-resolution STM image showing detailed appearance of upper and lower terraces, and nucleation of islands adjacent to line defects. Note the "specked" appearance of the surface due to admixture of P and Si atoms on both the islands and the underlying substrate. $V_{\text{sample}} = -2.0$ V, $I_{\text{tunnel}} = 0.2$ nA. Dimensions are 340×365 Å^2. (b) Atomic-resolution STM image showing detailed appearance of line defects and the characteristic appearance of P—P dimers and P—Si dimers. The highest terrace is labeled "1," the main large terrace labeled "2," and the lowest terrace is labeled "3." $V_{\text{sample}} = -2.0$ V, $I_{\text{tunnel}} = 0.2$ nA. Dimensions are 173×170 Å^2.

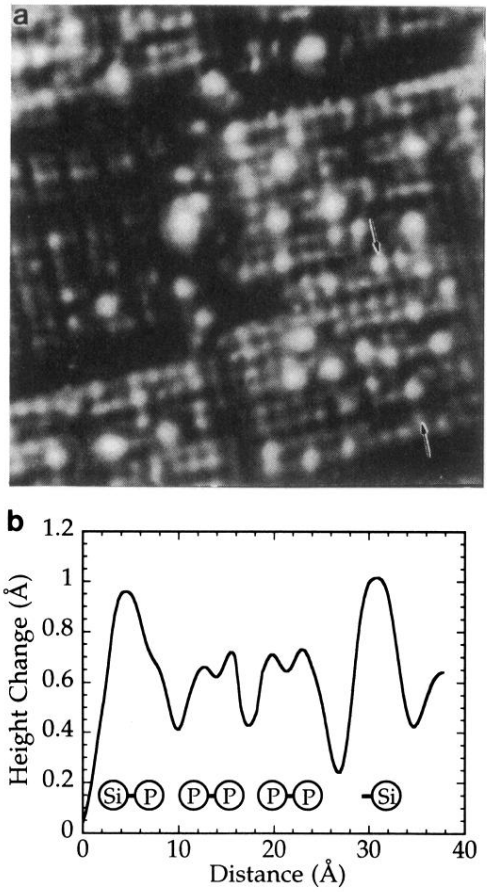

FIG. 3. (a) Enlarged image from Fig. 2(b), showing the appearance of P—P dimers as individual atoms, and showing that in Si—P dimers the Si atom appears as a high protrusion on one side of the dimer, with 50% probability of being found on either side. $V_{\text{sample}} = -2.0$ V, $I_{\text{tunnel}} = 0.2$ nA. Dimensions are 92×92 Å^2. (b) Height profile measured between the arrows indicated in Fig. 3(a), showing that P═P dimers appear as two protrusions with maxima separated by 3.2 Å, and Si "dangling bonds" on Si—P dimers appear about 0.3 Å higher.

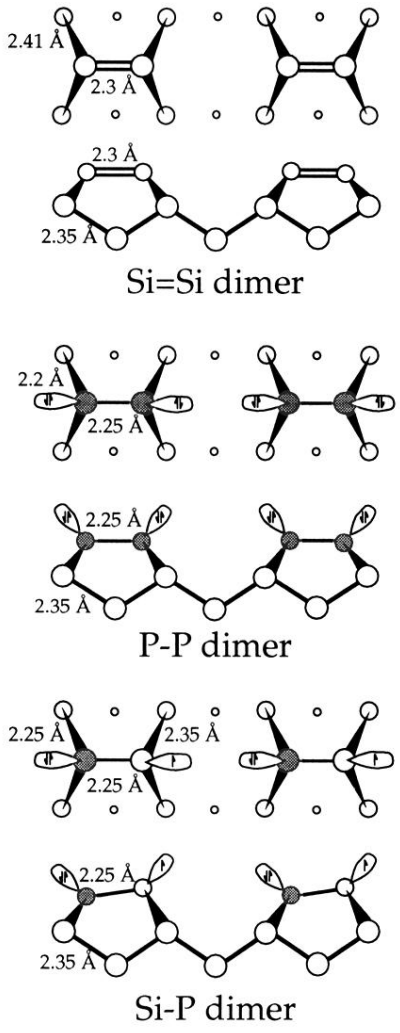

FIG. 4. Structural models for Si=Si, P=P, and Si—P dimer, including top and side views. Bond lengths are taken from the literature as described in the text.

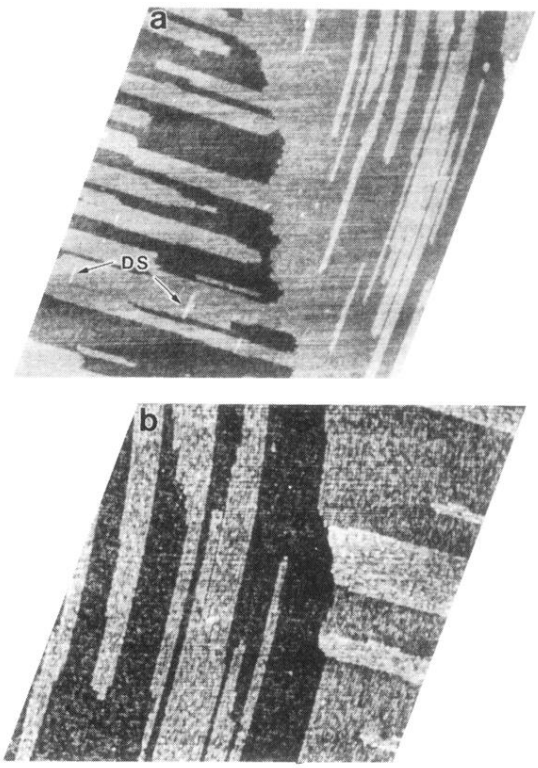

FIG. 7. (a) Large-scale STM image of surface partially covered by phosphorus, prepared as discussed in the text. Again note the formation of large anisotropic islands, but the absence of line defects. $V_{\text{sample}} = -2.15$ V, $I_{\text{tunnel}} = 0.2$ nA. Dimensions are 1250×1180 Å^2. (b) Higher-resolution STM image of partially P-terminated surface showing formation of highly anisotropic islands and the speckled appearance due to the mixture of Si=Si, Si—P, and P—P dimers. Note that the width of islands are no longer constrained by line defects. $V_{\text{sample}} = -2.15$ V, $I_{\text{tunnel}} = 0.2$ nA. Dimensions are 625×575 Å^2.

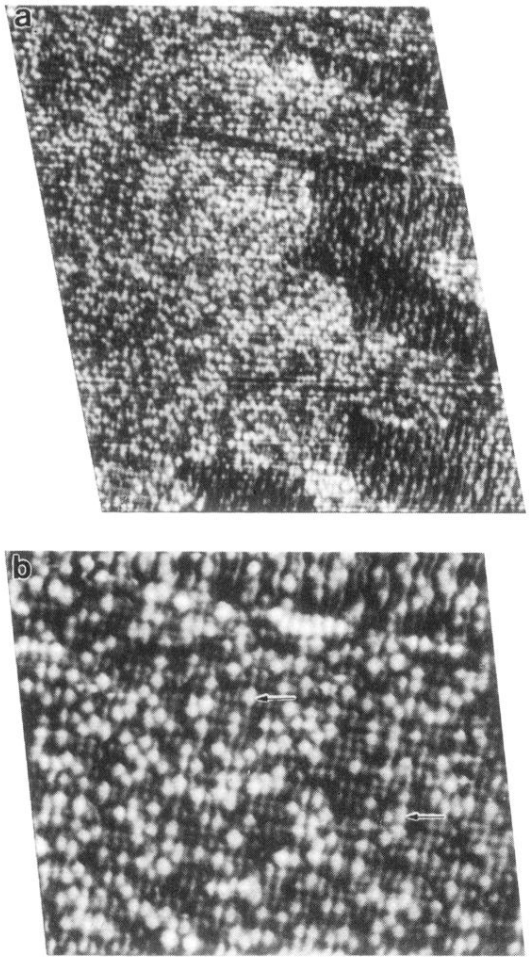

FIG. 8. (a) High-resolution STM image of partially P-terminated surface showing P—P and Si—P dimers; the chemical composition of the lower and upper terrace is the same. $V_{\text{sample}} = -2.2$ V, $I_{\text{tunnel}} = 0.2$ nA. Dimensions are 345×410 Å^2. (b) High-resolution image of partially P-terminated surface showing Si=Si, Si—P, and P—P dimers. Some Si=Si dimers are indicated with arrows; Si—P and P—P dimers can be found in numerous locations. There is a step edge near the top of the image. $V_{\text{sample}} = -2.2$ V, $I_{\text{tunnel}} = 0.2$ nA. Dimensions are 170×145 Å^2.